PAUL SCHERRER INSTITUT	SLS 2.0
Title Emittance exchange by coupling resonance crossing in the SLS booster synchrotron	Document identification SLS2-KJ81-003-1
Author(s) J. Kallestrup	February 23, 2021

1 Introduction

A horizontal off-axis injection scheme based on a 4-kicker bump is foreseen for the SLS 2.0 upgrade. The horizontal storage ring acceptance required to capture an incoming injection beam is sketched in Fig. 1 and is given by the equation

$$A_x = N_s \sqrt{\beta_{x,s} \epsilon_{x,s}} + 2N_i \sqrt{\beta_{x,i} \epsilon_{x,i}} + S, \tag{1}$$

The acceptance required can be minimized by either i) decreasing the septum blade thickness, S, or ii) decreasing horizontal emittance, $\epsilon_{x,i}$. The SLS booster provides a beam with horizontal emittance of $\approx 12\,\mathrm{nm}\,\mathrm{rad}$ at 2.7 GeV, which can be injected without losses into the storage ring acceptance [1]. However, further headroom for the injection can be provided in case of reduced dynamic aperture by using performing an emittance exchange of the booster beam. In doing emittance exchange, the large horizontal emittance is exchange with the small vertical emittance, whereby effectively decreasing ϵ_x . At the SLS booster, we do emittance exchange by crossing the linear coupling resonance:

$$\Delta = Q_x - Q_y - \ell = 0. \tag{2}$$

Doing this correctly will lead to a complete exchange of the emittances. The physics behind this process and the first demonstration at the SLS booster was published in [2]. In the remainder of this note we list some details about the practical implementation.

2 Emittance exchange implementation

The SLS booster has a working point around $(\widehat{Q}_x, \widehat{Q}_y) = (0.46, 0.36)$ during user operation, giving a tune separation of $\Delta = 0.1$. The tunes measured along the full booster ramp are plotted in Fig. 2a. The objective is to cross the linear coupling resonance, i.e. the fractional part of the tunes must cross each other. To do so, we have three quadrupole families available:

i) QF:
$$\beta_x = 10.1 \,\mathrm{m}$$
, $\beta_y = 2.6 \,\mathrm{m}$. $k_1 \ell = 0.61 \,\mathrm{m}^{-1}$,

ii) QD:
$$\beta_x = 4.2 \,\mathrm{m}$$
, $\beta_y = 4.1 \,\mathrm{m}$. $k_1 \ell = -0.29 \,\mathrm{m}^{-1}$,

iii) QE:
$$\beta_x = 1.6 \,\mathrm{m}$$
, $\beta_y = 10.15 \,\mathrm{m}$. $k_1 \ell = -0.02 \,\mathrm{m}^{-1}$.

The magnetic ramps of the three family power supplies in user operation are plotted in Fig. 3. To do resonance crossing we cannot easily use the QD family, since increasing/decreasing the family will move both tunes in the same direction. The QE family is weakly excited in normal operation. Furthermore it is the only dipolar supply of the three families, making it ideal for adjusting Q_x without much impact to Q_x . Lastly, the QF family allows for adjustment of Q_x with little impact on Q_y .

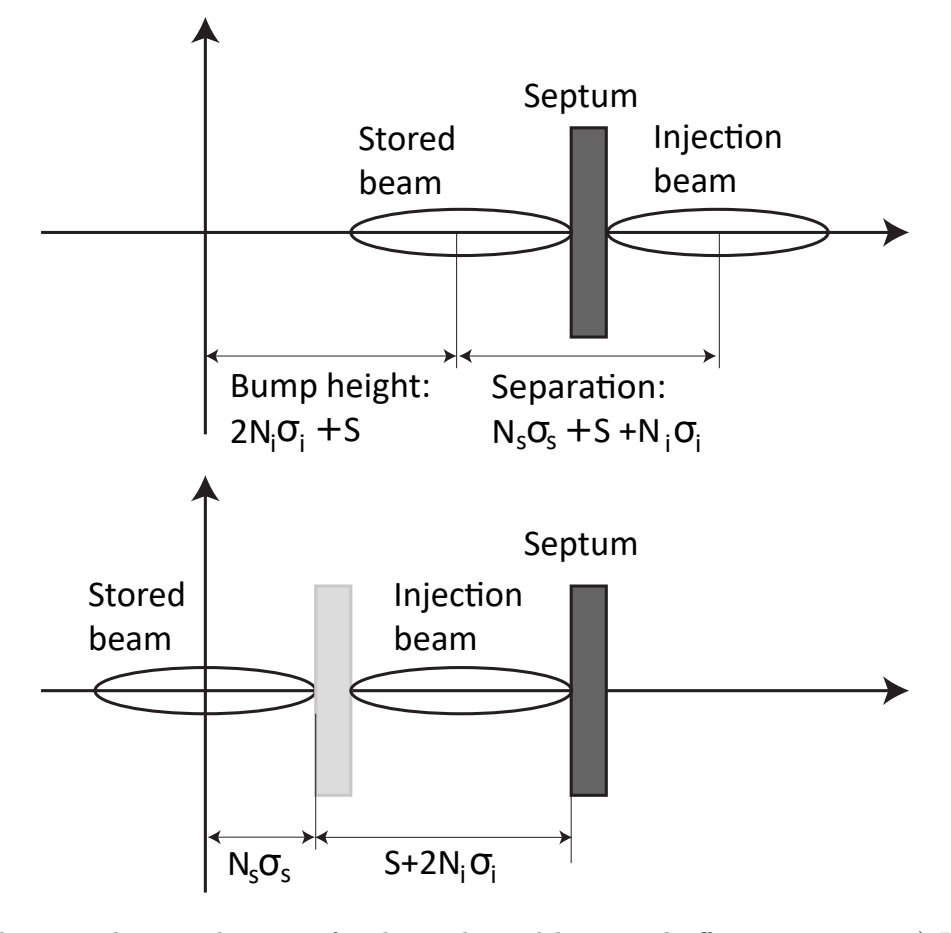


Figure 1: Schematic showing the setup for the traditional horizontal off-axis injection. a) Kicker bump on during injection. b) Kicker bump off after injection. Minimizing the horizontal emittance of the injected beam will greatly reduce the required aperture. In this figure, the orbit bump height is minimal: it can be higher if the kicker bump is stronger but not lower.

Now, three options for resonance crossing can be imagined:

- a) Moving Q_x to cross Q_y using the QF family,
- b) Moving Q_y to cross Q_x using the QE family,
- c) Moving Q_x and Q_y simultaneously using the QF and QE families.

The three crossings are illustrated in the tune diagram on Fig. 4 (here only with a few additional resonances, and made with symmetric distance to the coupling resonance ($\Delta=\pm 0.1$ before/after the crossing) for convenience). Moving Q_y only is not an option, since we would end up close to- or even crossing the half-integer resonance. Moving both Q_x and Q_y is ideal, since the distance in the tune space diagram is the shortest. It, however, requires two quadrupole families simultaneously which adds a bit of complexity in the brute-force adjustment of the ramps (see later). Therefore, we have generally used option a) to move only Q_x with the QF family, as our base concept.

The next thing to check is the coupling of the machine. The best way of quantifying coupling is through the coupling coefficient:

$$C = -\frac{1}{2\pi} \oint ds K_s \sqrt{\beta_x(s)\beta_y(s)} e^{-i\left[\phi_x(s) - \phi_y(s) + \frac{s}{R}\Delta\right]},\tag{3}$$

where K_s is the skew quadrupole component at location s, $\beta_x(s)$ and $\beta_y(s)$ are β -functions in the horizontal and vertical planes at location s, respectively, R is the average radius of the machine. Knowing the coupling

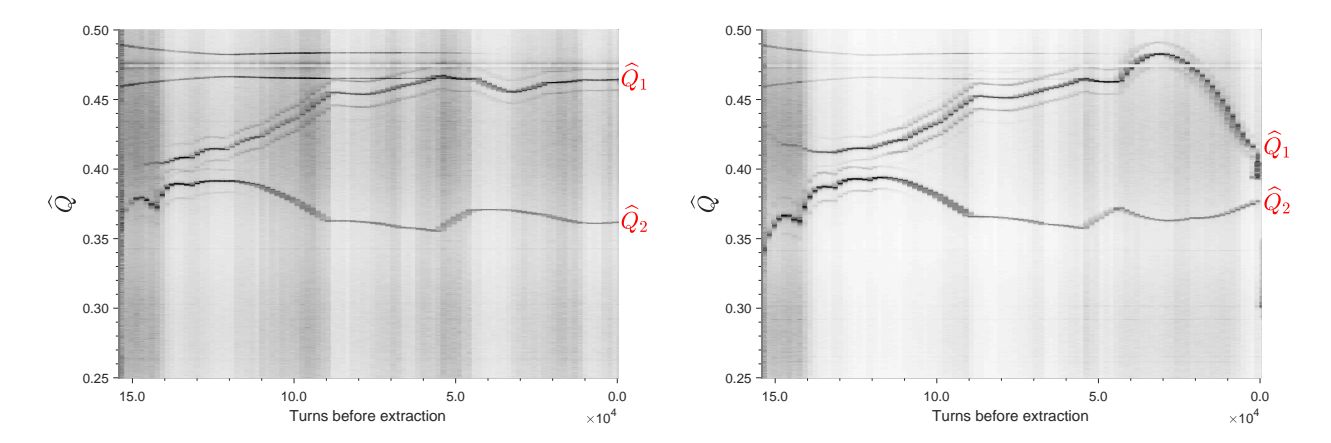


Figure 2: FFT spectra of turn-by-turn beam position after coherent betatron oscillations are excited by a kicker as a function of turns before extraction. The measured tunes are visible as black lines.

coefficient is important, since it influences the emittance sharing for a given working point. For example, if $\Delta = 0.04$ and |C| = 0.001, then the sharing of the horizontal emittance into the vertical plane (without emittance exchange!) is much smaller than if |C| = 0.01. This can be found through the equation (for undamped beams)

$$\epsilon_x = \epsilon_{x,0} + \frac{|C|^2}{\Delta^2 + |C|^2} \frac{(\epsilon_{y,0} - \epsilon_{x,0})}{2}, \epsilon_y = \epsilon_{y,0} - \frac{|C|^2}{\Delta^2 + |C|^2} \frac{(\epsilon_{y,0} - \epsilon_{x,0})}{2}.$$
 (4)

So to achieve a good emittance exchange, it is important that $\Delta \gg |C|$ before the exchange to avoid emittance sharing, and after to ensure completeness of the exchange.

When measuring the tunes of a machine with non-zero coupling, one does not find \widehat{Q}_x and \widehat{Q}_y . Instead, the normal mode tunes, Q_1 and Q_2 , are measured due to the finite coupling

$$Q_{1,2} = Q_{x,y} \mp \frac{1}{2}\Delta \pm \frac{1}{2}\sqrt{\Delta^2 + |C|^2},\tag{5}$$

with |C| being the amplitude of the coupling coefficient. This equation reveals that the normal mode tunes cannot cross each other; when $\Delta=0$ (i.e. $\hat{Q}_x=\hat{Q}_y$) we have $\hat{Q}_1-\hat{Q}_2=|C|$, and the normal mode tunes are separated by a finite stop band of size |C|. The amplitude of the coupling coefficient can therefore be measured from the minimum separation of the fractional parts of the normal mode tunes by step-wise changing the tunes with quadrupoles. This method is commonly known as the closest-tune approach. We measure |C| by adjusting the peak value of the QF family in several steps from 99.3 A to 97.25 ${\bf A}^1$ and measure the tunes as described earlier. The horizontal and vertical tune peaks found are plotted in Fig. 5. The smallest separation of the fractional tunes is $|C|\approx 0.019$, which is a rather large value. Based on this result, we decide to attempt the resonance crossing by decreasing the QF family current from $I_{\rm QF}=98\,{\rm A}$ to $I_{\rm QF}=95\,{\rm A}$. However, the nominal QF value is $I_{\rm QF}=99.75\,{\rm A}$, and so we add a small flat-top to the QF ramp. Adding the flat-top makes Q_1 go slowly towards Q_2 without performing the crossing. This is seen at the end of the ramp in Fig. 2b. The resonance crossing itself is implemented as a rapid decrease in $I_{\rm QF}$ at the very end of the ramp. The QF ramps before/after the modifications are plotted in Fig. 6.

2.1 Analyzing the exchange process

After having downloaded and enabled a set of quadrupole ramps, it is easy to verify by eye that some emittance exchange has been performed simply by visually checking the image on screen monitors in the booster-to-ring transfer line with/without the adjusted quadrupole ramps. Two examples of the beam profile on the ABRDI-SM-3 monitor before/after the resonance crossing is shown in Fig. 7. However, the quality of the emittance exchange can deteriorate due to radiation damping or too fast resonance crossing (the latter is shown in more detail in

¹Quadrupole currents reported here are without adding the injection set-point of 2.475 A value to the calculation. This must be done if the injection set-point is modified later on.

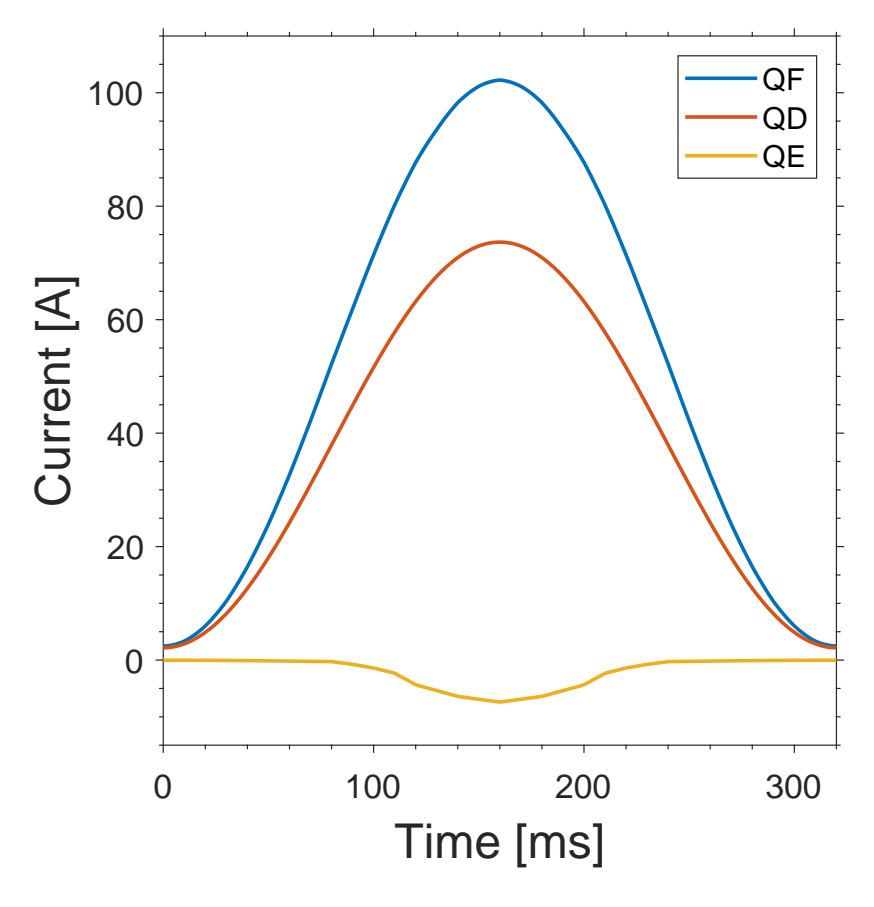


Figure 3: Magnetic ramps of the QF (blue), QD (red) and QE (yellow) quadrupole power supplies.

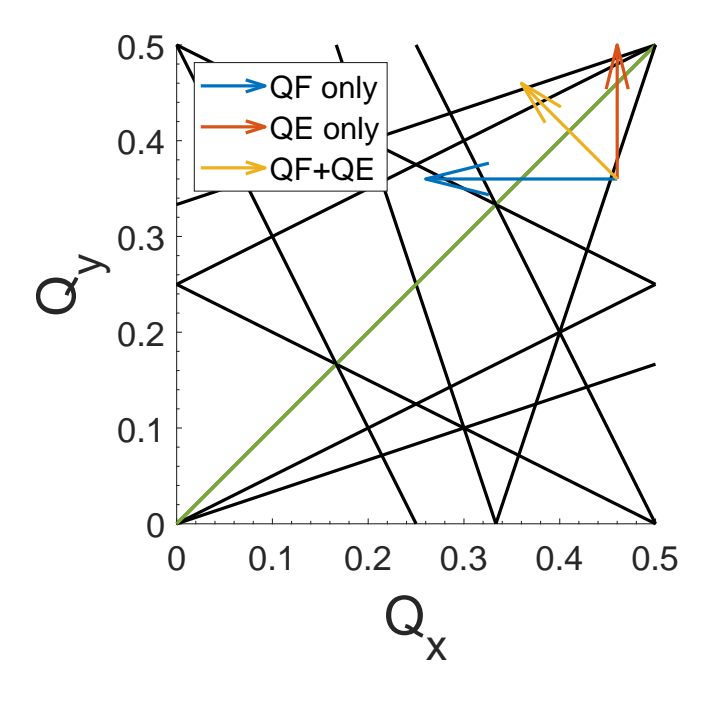


Figure 4: Tune space plot with three options for resonance crossing for the SLS booster working point. A fixed tune distance before/after the crossing is used for visualization

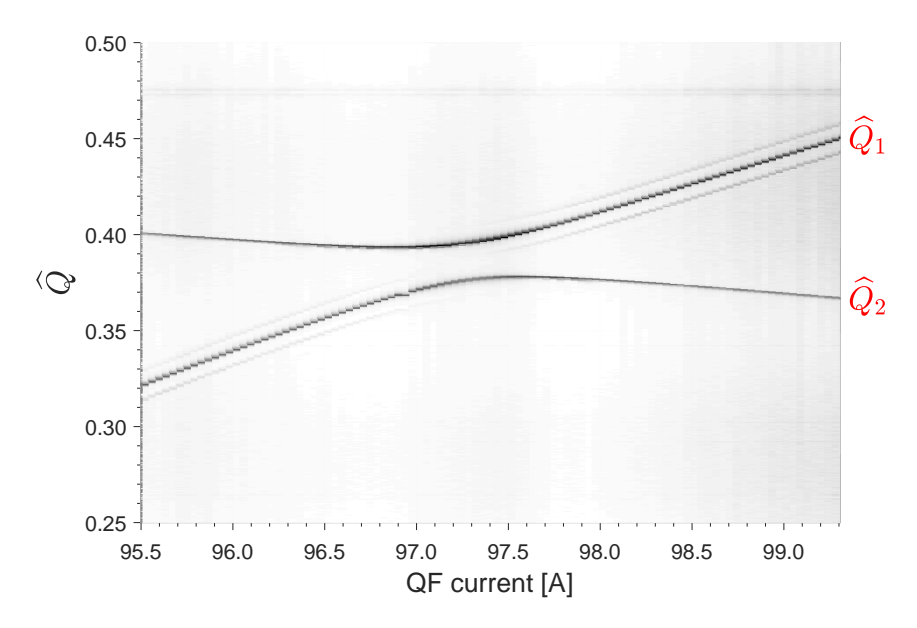


Figure 5: FFT of beam motion at the top of the ramp for different currents of the QF family. The horizontal fractional normal mode tune changes from 0.325 to 0.450 when changing the QF current from $I_{QF}=95.5\,\mathrm{A}$ to 99.3 A. The smallest tune separation is reached around $I_{QF}=97.25\,\mathrm{A}$ revealing a coupling coefficient amplitude of |C|=0.019

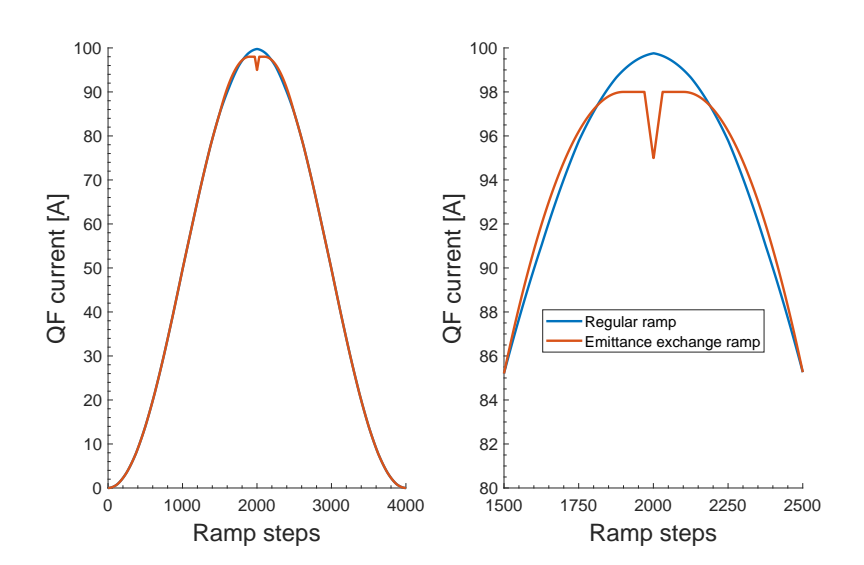


Figure 6: QF-quadrupole family ramp to achieve emittance exchange. Nominal ramp is also shown for comparison. A short flat-top at 98 A is followed by a quick drop to 95 A over the last 30 ramp steps, leading to coupling resonance crossing. Left: Full ramp comparison. Right: Zoom of the modified part of the ramp.

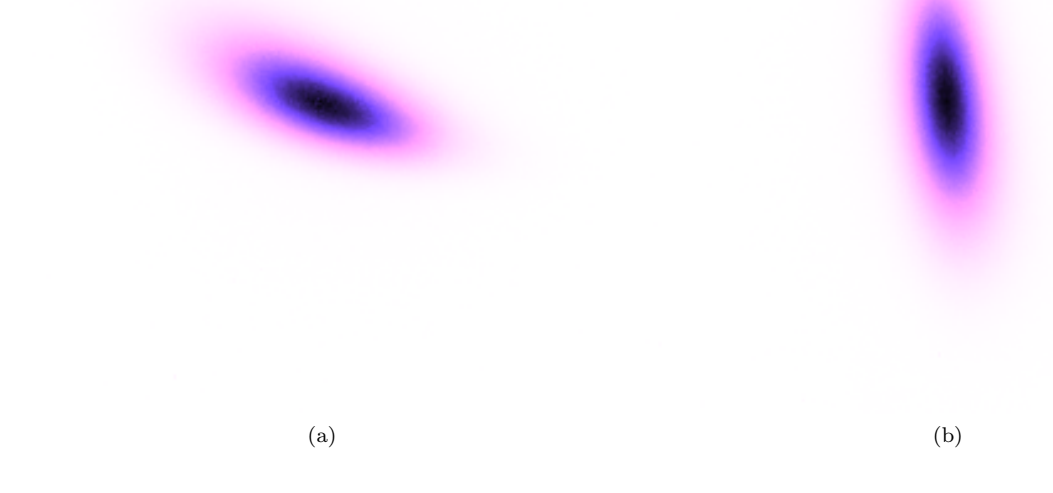


Figure 7: Beam profiles on the ABRDI-SM-3 monitor using emittance exchange a) 2000 turns before normal extraction time (before resonance crossing) b) at normal extraction time (after resonance crossing). Note that these pictures are taken with transfer line optics set such that $\beta_x = \beta_y = 80 \,\mathrm{m}$ (assuming design optics at the entrance to the transfer line) for visualization of the emittance exchange only, and does therefore not correspond to the design BRTL settings. However, the resonance crossing is identical.

Sec. 3). The best way of checking optimality of the emittance exchange is by performing a measurement of how the beam sizes changes during the emittance exchange process. At the SLS booster we do this by extracting the beam to the booster-to-ring transfer line during the exchange process by shifting the extraction kicker timing and then measuring the profile on a screen monitor. A such plot for the above described resonance crossing is shown in Fig. 8. The effect of the emittance exchange is clearly seen. The horizontal beam size is decreased by a factor ≈ 2 . Subtracting measured dispersion leads us to conclude that the horizontal emittance is decreased by a factor 4.2 and the vertical increased with approximately same factor.

2.2 Improved emittance exchange

In hind sight, the starting point of the resonance crossing ($I_{\rm QF}=98\,{\rm A}$) was too close to the resonance to begin with for the large value of $|C|\approx 0.019$. This can also be seen by visual inspection of Fig. 7a as a clear tilt of the beam. This, together with the decoupling of transverse planes and associated vertical beam size decrease [4], lead to a quite significant improvement to the emittance exchange, as is shown in Fig. 9. The horizontal beam size after the emittance exchange is now further decreased by a factor ≈ 2 compared to the previous result of Fig. 8. It is important to note that since the horizontal emittance is essentially unaffected of the vertical beam size minimization, the vertical beam size after the emittance exchange is approximately the same as before the minimization.

3 Non-adiabatic crossing due to low coupling

The best possible emittance exchange is achieved in the situation where the particles do not emit synchrotron radiation, and where the resonance is crossed infinitely slowly. Since this is not a realistic situation, one may run into a situation where the resonance is crossed too quickly, leading to incomplete emittance exchange. A such resonance crossing is called "non-adiabatic". A simple simulated example is shown in Fig. 10a. Non-adiabaticity

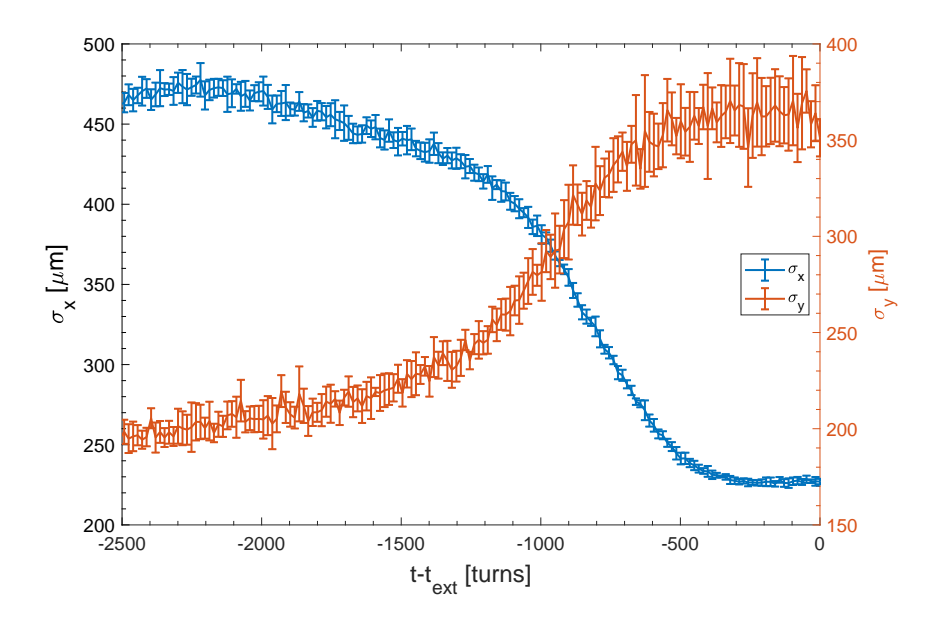


Figure 8: Beam size measurements for various extraction kicker delays. The beam sizes are measured with an OTR screen installed in the Booster-to-Ring Transfer line.

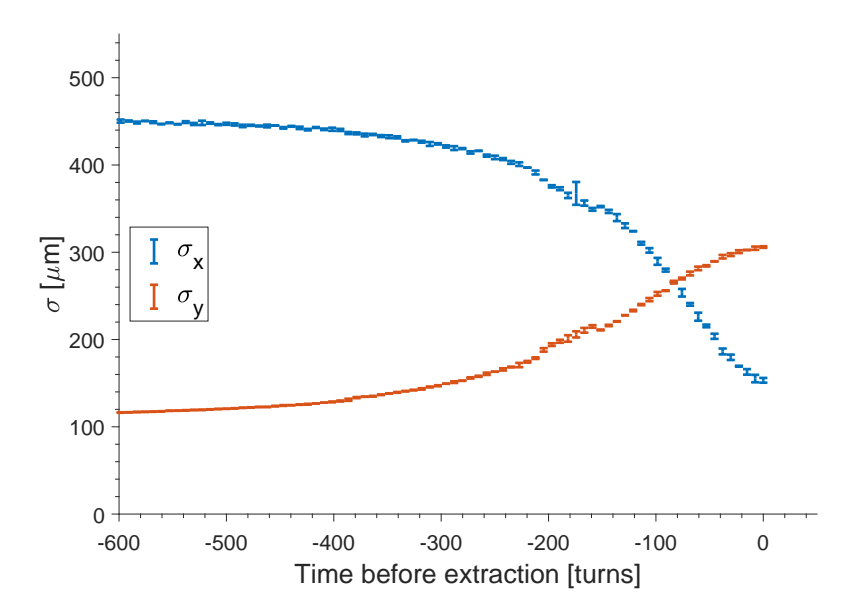


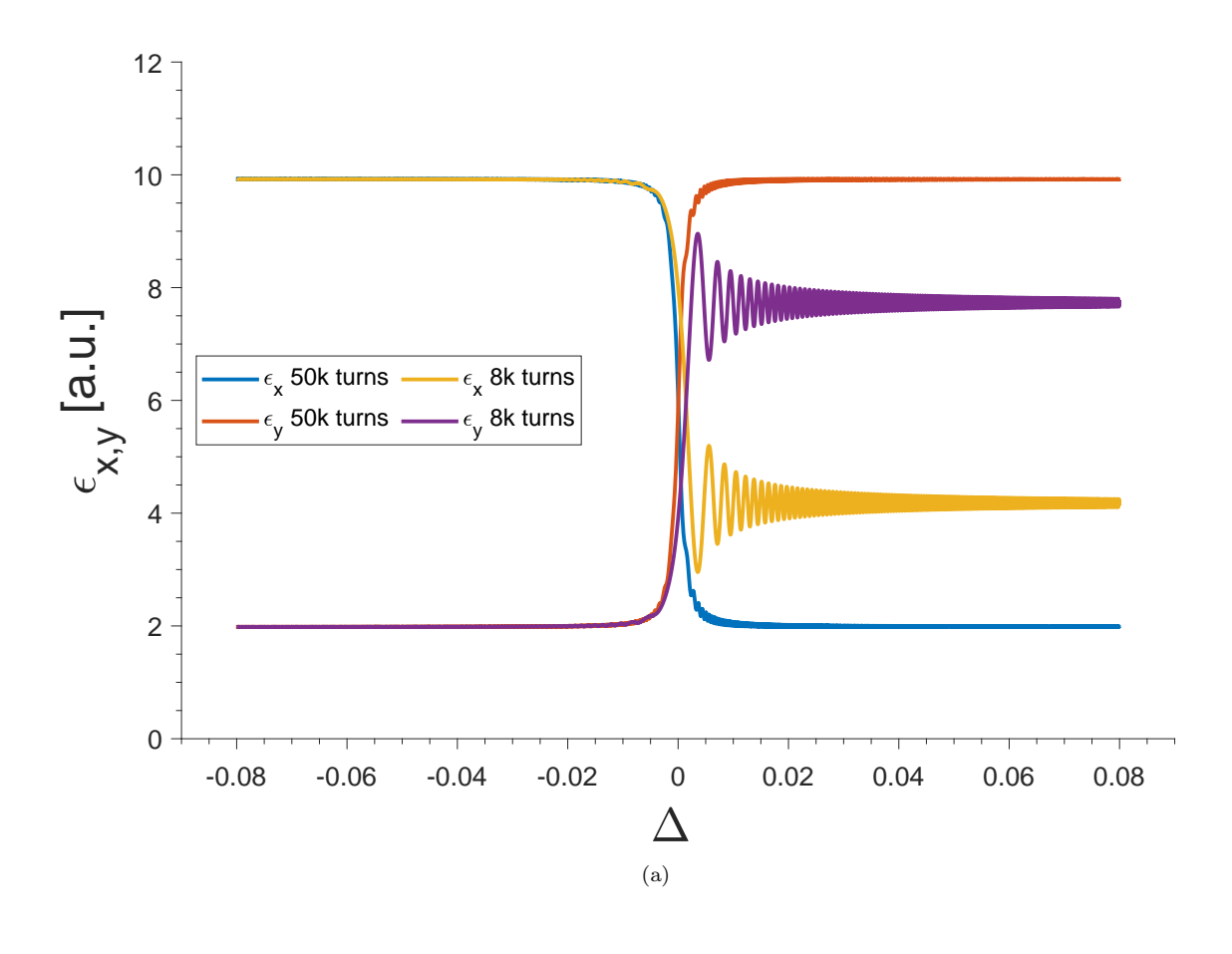
Figure 9: Beam size measurements for various extraction kicker delays after optimizing the beam quality and emittance exchange procedure. The beam sizes are measured with an OTR screen installed in the Booster-to-Ring Transfer line.

is investigated in detail in [2] and [3]. A non-adiabatic crossing is typically encountered if the coupling of the machine (quantified by the coupling coefficient |C|) is too small. In [4] we performed a vertical beam size minimization, leading to a factor 10 decrease of |C|. Performing emittance exchange under those conditions can be tricky. An example of a non-adiabatic exchange in the SLS booster is given in Fig. 10b.

Performing a measurement like in Fig. 10b clearly reveals the cause of an incomplete emittance exchange: if the resonance crossing is non-adiabatic the beam sizes will be show out-of-phase oscillatory behavior, while if synchrotron radiation is dominant, we will see a gradual deterioration.

References

- [1] A. Streun, "SLS 2.0 Baseline Lattice", SLS note: SLS2-SA81-004-16
- [2] J. Kallestrup and M. Aiba, "Emittance exchange in electron booster synchrotron by coupling resonance crossing", Phys. Rev. Accel. Beams 23, 020701 (2020)
- [3] M. Aiba and J. Kallestrup, "Theory of emittance exchange through coupling resonance crossing", Phys. Rev. Accel. Beams 23, 044003 (2020)
- [4] J. Kallestrup, "Vertical beam size minimization in the SLS booster", SLS note: SLS2-KJ81-001-1
- [5] J. Kallestrup, "SLS booster fast head-tail instability characterization and cure", SLS note: SLS2-KJ81-002



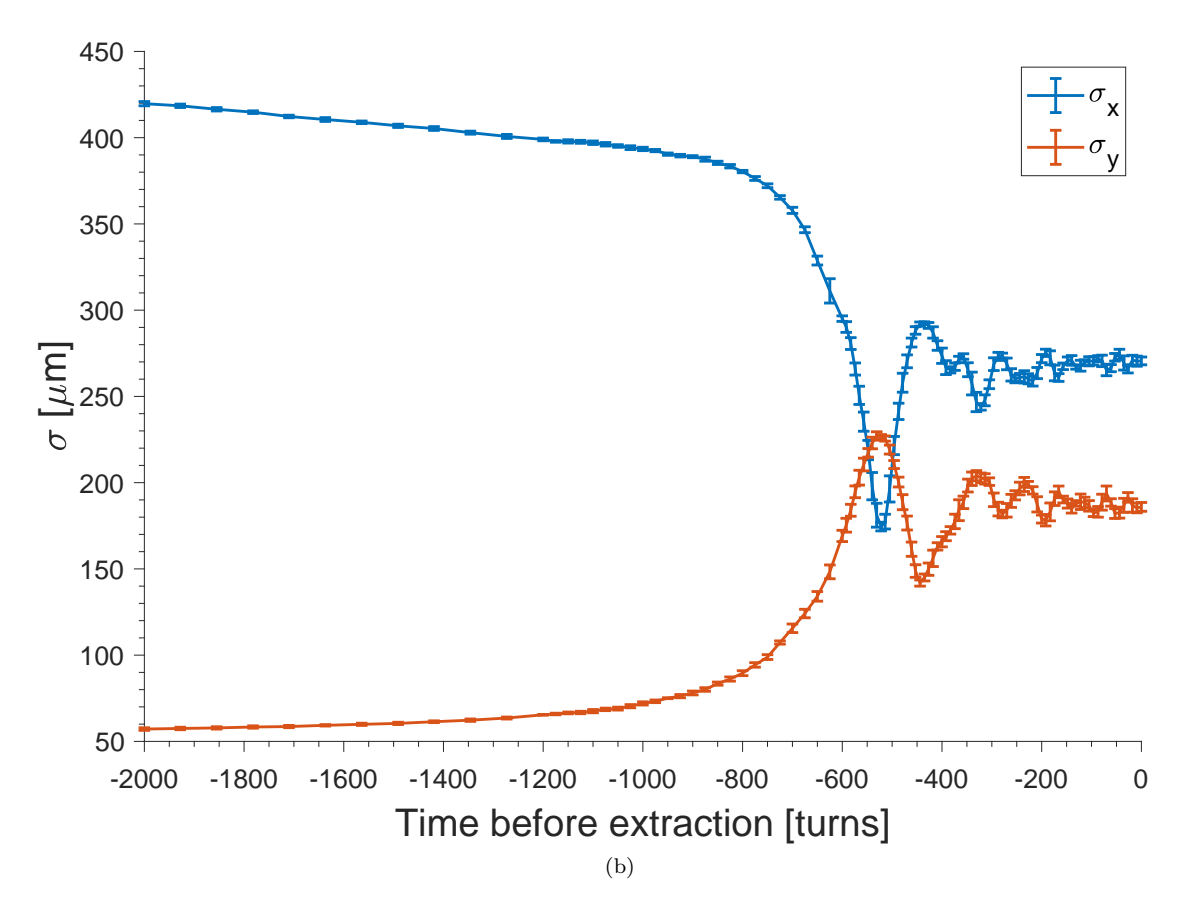


Figure 10: Examples of non-adiabatic emittance exchanges in a) simple simulation b) measurement in the SLS booster.